

Photon Production from a Quark–Gluon Plasma

E.Quack* and P.A.Henning†

Theory Group, Gesellschaft für Schwerionenforschung (GSI)

P.O.Box 110552, D-64220 Darmstadt, Germany

(January 5, 1996, GSI-Preprint 95-42 (revised), hep-ph 9507273)

Abstract

In-medium interactions of a particle in a hot plasma are considered in the framework of thermal field theory. The formalism to calculate gauge invariant rates for photon and dilepton production from the medium is given. In the application to a QED plasma, astrophysical consequences are pointed out. The photon production rate from strongly interacting quarks in the quark–gluon plasma, which might be formed in ultrarelativistic heavy ion collisions, is calculated in the previously unaccessible regime of photon energies of the order of the plasma temperature. For temperatures below the chiral phase transition, an effective field theory incorporating dynamical chiral symmetry breaking is employed, and perturbative QCD at higher temperatures. A smooth transition between both regions is obtained. The relevance to the soft photon problem and to high energy heavy ion experiments is discussed.

Typeset using REVTeX

*Present address: Theory Group, SLAC, Stanford University, P.O. Box 4349, Stanford, CA 94309, USA; email: quack@slac.stanford.edu

†e-mail: P.Henning@gsi.de

I. INTRODUCTION

Considerable effort is invested in present and future experiments of ultrarelativistic heavy ion collisions (URHIC) in order to observe an excursion of the bulk of strongly interacting matter from the state of hadrons before the collision into the phase of a quark–gluon plasma (QGP) [1]. In order to see this shortlived state directly, one would like to observe photons emitted from the hot plasma, as well as dileptons. Since these probes interact only electromagnetically, their signal is not distorted by later interactions as are other particles which are studied for the same purpose.

The experimental capability of measuring electromagnetic probes was demonstrated in the photon channel by Helios [2], WA80/98 [3] and CERES [4] as well as in the dilepton channel by Helios [5] and CERES [6].

The signal originating from the plasma phase is, however, buried under a background of photons from different origin such as from the decays of π^0 or η or from hadronic reactions at a temperature comparable to that of the deconfined phase [7]. After subtraction of these sources, a remaining signal seems to persist in part of the experimental analysis. At present, it is vividly discussed to what extent one can account for these data within more [8] or less [9] conventional physical pictures.

However, our theoretical knowledge of the spectrum of electromagnetic probes from both the plasma as well as the hadronic phase is still uncertain to some extent. A better handle on these spectra from theoretical calculations is necessary in order to disentangle the various sources and to identify the phases reached during the collision. In particular for the soft part of electromagnetic radiation, this problem represents a challenge to theory in itself, due to the nonperturbative nature of the photon emission process: Multiple rescattering of the emitting particles and the Landau-Pomeranchuk-Migdal (LPM) effect play an important role in the medium for photon energies $E_\gamma \leq T$ [10,11], as well as for dileptons of an invariant mass in this range.

This problem motivated the present work, in which we will investigate the production of photons and dileptons from a strongly interacting plasma at finite temperature. After a short sketch of the insufficiencies of existing calculations, we show how one can reach an improvement by taking thermal scattering and thereby spectral broadening of the emitting particles in the heat bath into account. The problem is addressed in the framework of thermal field theory, results are given for a QED plasma as well as for a QGP within a model incorporating dynamical chiral symmetry breaking. A part of the results has been presented already in a short paper [12].

In an α_s expansion, the lowest order of photon production proceeds via annihilation ($q\bar{q} \rightarrow g\gamma$) and Compton ($qg \rightarrow q\gamma$) processes. In next to leading order (NLO), numerous corrections to these processes arise, a complete calculation of the order $\mathcal{O}(\alpha\alpha_s^2)$ has been achieved in [13]. With an initial quark and gluon distribution specified by distribution functions $f_1(E_1)$ and $f_2(E_2)$, and the final state quark or gluons distribution $f_3(E_3)$, the production rate reads

$$R^0 = E \frac{dN_\gamma^0}{d^3\mathbf{p}}$$

$$= \mathcal{N} \int \sum_{i=1}^4 \frac{d^3 \mathbf{p}_i}{2E_i (2\pi)^3} f_1(E_1) f_2(E_2) (2\pi)^4 \delta^4(p_1 + p_2 + p_3 - p_4) |M|^2 [1 \mp f_3(E_3)] , \quad (1)$$

where the last factor takes into account Pauli blocking or Bose enhancement of the quark or gluon in the final state, and M stands for the elementary cross section considered.

The production of hard (high p_\perp) photons in reactions of colliding hadrons has been calculated using ‘cold’ parton distributions delivered by structure functions and using M in NLO. For sufficiently high p_\perp , very good agreement with the corresponding data is reached [14], only towards low p_\perp some discrepancy has been reported [15]. This may hint at the insufficiency of using even NLO calculations in the soft regime, but may equally well be due to our still insufficient knowledge of the parton distribution functions in the relevant x and Q^2 range, see [16] for an analysis. Even with this minor uncertainty, one has reached a very good quantitative understanding of photon production.

Now let us look at the same processes in a plasma, where the partons have reached a thermal distribution. We will consider situations in which the spatial extension of the plasma is lower than the mean free path of the photons emitted, i.e. we consider the emission of ‘white’ radiation in contrast to thermal black body radiation. Due to the small size of nuclei compared to the mean free path of an electromagnetically interacting particle, this is always the case for heavy ion collisions. Using M in lowest order, and taking thermal quark (q), \bar{q} and gluon distributions of temperature T results in a production rate R (per unit volume element) as [17]

$$R^0 = E \frac{dN_\gamma^0}{d^3 \mathbf{p}} = \frac{5}{9} \frac{\alpha \alpha_s}{2\pi^2} T^2 e^{-E/T} \left[\log \frac{ET}{m^2} + c^0 \right] \quad (2)$$

with some constant c^0 . This rate diverges when $m \rightarrow 0$, which is the crucial limit of chiral symmetry restoration for strongly interacting quarks approaching the phase transition temperature. This unphysical divergence will eventually be shielded by medium effects on the emission process.

A step towards the calculation of such medium effects has been the application of the Braaten–Pisarski method of hard thermal loops [18] to this problem [7,19]. The resulting photon production rate is

$$R^{\text{BP}} = E \frac{dN_\gamma^0}{d^3 \mathbf{p}} = \frac{5}{9} \frac{\alpha \alpha_s}{2\pi^2} T^2 e^{-E/T} \log \frac{c_1 E}{g^2 T} \quad (3)$$

with a constant $c_1 \sim 3$ and the strong coupling constant g . For $g^2 \sim c_1$, the term $\log(E/T)$ reminds us of the validity of this approach only in the region of $E_\gamma \gg T$.

A more detailed investigation of this infrared problem within the hard thermal loop (HTL) method of Braaten and Pisarski has been presented in [20,21]. In these works, the production of soft photons was studied thoroughly. The origin of the infrared problem could be traced back to divergences which occur when the real photon is emitted collinear to a thermal gluon. For this reason, it was concluded in [20,21] that no finite value for the production rate of soft photons can be obtained within the HTL method.

This is the motivation for the present work. Physically, the HTL method takes into account the thermal masses particles acquire in the medium. In addition to that, we now

also consider the thermal scattering of the partons, which results in an energy uncertainty as the quark propagates. As we will show below, this is the dominant physical process to be considered for quarks emitting soft photons with energies $E_\gamma \leq T$. The thermal scattering leads to a finite lifetime (or nonzero spectral width) of every excitation in the medium, described in analogy to the decay width of an excited state [22]. One effect of such a spectral width is that it naturally removes the infrared divergences mentioned before, therefore enables us to calculate production rates for soft photons. Secondly, the energy “uncertainty”, which is actually a kind of Brownian motion, is directly related to the emission rate of thermal photons.

This paper is organized as follows. In the next section, we present the general formalism of thermally scattered particles in a heat bath. This includes the calculation of thermal widths as well as the photon production rate in a gauge invariant manner. Section II.C gives the comprehensive example of a fermion (quark) in a QED plasma. Although not being realistic for the QCD case, it allows for simpler and often analytic solutions and thus for a clear illustration of the relevant physics.

We then turn to the case of the QCD plasma, section III. A crucial aspect of QCD at low temperatures is the breaking of chiral symmetry. Hence up to the chiral phase transition temperature we describe the plasma by the Nambu–Jona-Lasinio model, which incorporates this feature dynamically (Sect. III.A). In the subsequent part of this work, III B, we turn to high-temperature perturbative QCD, with temperature dependent strong coupling constant α_s . Section III.C gives the results for the photon production rates over the entire range of temperatures and of photon energies, and we discuss the relevance to a variety of experimental situations in section III.D.

II. PHOTON RADIATION IN THERMAL FIELD THEORY

In this section, we first briefly recall the formalism of thermal field theory using spectral functions, outline how the self energy of a thermal particle is obtained in general, how it is related to the thermal width and how gauge invariant rates for photon production are obtained therefrom. We finally illustrate the achievements with the example of a fermion in a QED plasma.

A. Spectral functions and self energies

For any physical system one would like to have a *causal* description: Physical particles e.g. may exert a measurable influence only after their emission. In the framework of quantum field theory this means that one would like to use causal Green functions or propagators in the theoretical description. The requirement of causality however touches two aspects of field theory. It relates the boundary condition in time that a propagator fulfills to the average occupation number of the state that is propagated.

For a vacuum state, this leads to the well-known Feynman boundary conditions, which in terms of the free propagator in momentum state translate into the simple $+i\epsilon$ -description in the denominator.

At nonzero temperature, the average occupation number of a state is given by a thermal equilibrium distribution function (Bose-Einstein or Fermi-Dirac). Hence, the temporal boundary conditions for the propagation of particles at finite temperature are more complicated than in a vacuum state, they are called the Kubo-Martin-Schwinger (KMS) condition [23].

This KMS condition leads to a causal propagator with a complicated analytical structure. It is therefore safer for thermal systems to deviate from the description in terms of causal propagators. Rather one uses only retarded and advanced propagators, whose temporal boundary conditions do not depend on the occupation number of states. It is well known, how to express a finite temperature perturbation theory in terms of retarded and advanced propagators (see refs. [24,25] for an extensive discussion).

Mathematically, the retarded and advanced propagators are analytical functions of their energy parameter in the upper or lower complex half-plane. Analytical functions however obey the Kramers-Kronig relation, and this implies that the retarded propagator of an interacting field theory is known completely if only its imaginary part (or spectral function) \mathcal{A} is known along the real axis. Hence, for the retarded quark propagator in our system we write, for arbitrary complex energy E

$$S^{R,A}(E, \mathbf{p}) = \int_{-\infty}^{\infty} dE' \mathcal{A}_q(E', \mathbf{p}) \frac{1}{E - E' \pm i\epsilon}. \quad (4)$$

For free particles the spectral function is proportional to a δ -function,

$$\mathcal{A}_q^{\text{free}} = (E\gamma^0 - \mathbf{p}\boldsymbol{\gamma} + m_q) \text{sign}(E) \delta(E^2 - \mathbf{p}^2 - m_q^2), \quad (5)$$

which kinematically limits the asymptotic states to be on-shell.

However, as we have argued above, such asymptotically stable states are not present in a finite temperature system: Each particle is subject to collisions which will add a statistical (thermal) uncertainty to its energy as function of time (thermal scattering, or Brownian motion). This indicates that the limit of a δ -like spectral function cannot be used in interacting thermal systems – which has been proven rigorously in the Narnhofer-Thirring theorem [22].

One may attribute this to a fundamental property of *temperature*: A thermal particle distribution function has a special rest frame, hence corresponds to a breaking of the Lorentz invariance. It is well-known that a state of broken symmetry requires to chose adequate basis functions for a quantization. In case of the finite temperature breakdown of Lorentz invariance, the basis functions turn out to be quantum fields without a mass shell [26,27]. In other words, the field theoretically correct way to treat a finite temperature system is in terms of *continuous* spectral functions.

How to put these two aspects together, i.e., the transformation to retarded/advanced propagation as well as the perturbative expansion in terms of generalized free fields with continuous mass spectrum, is discussed in ref. [25]. For the purpose of the present paper, it is sufficient to choose a parametrization for such a spectral function.

B. Parametrization of the quark spectral function

For this parametrization we take as a guideline the idea to be not too far from the quasi-particle picture, i.e., we make an ansatz for the inverse retarded quark propagator

$$p_\mu \gamma^\mu - m_q^0 - \Sigma^R(p) \approx (p_0 \pm i\gamma_q) \gamma_0 - \mathbf{p}\boldsymbol{\gamma} - m_q \quad (6)$$

with a given self energy function $\Sigma^R(p)$ in the vicinity of $p_0 = \pm \sqrt{\mathbf{p}^2 + m_q^2}$ and $|\mathbf{p}| \ll m_q$. This implies, that we assume the whole model to be dominated by its infrared sector, see the remark at the end of this subsection. This ansatz translates into a spectral function as

$$\mathcal{A}_q(E, \mathbf{p}) = \frac{\gamma_q \gamma_0 (E^2 + \Omega_q(\mathbf{p})^2) - 2E\boldsymbol{\gamma}\mathbf{p} + 2Em_q}{\pi (E^2 - \Omega_q(\mathbf{p})^2)^2 + 4E^2\gamma_q^2}. \quad (7)$$

Here, $\gamma_\mu = (\gamma_0, \boldsymbol{\gamma})$ is the four-vector of Dirac matrices and $\Omega_q(\mathbf{p})^2 = \mathbf{p}^2 + m_q^2 + \gamma_q^2$. m_q is the dynamical mass of the quark, and its spectral width parameter we label γ_q . Note however, that the half-maximum width of the spectral function peak is $2\gamma_q$.

One may regard this spectral function as the generalization of the standard energy-momentum relation of eq. (5) to a broader distribution for thermally scattered particles, in this particular case represented by a double Lorentzian. Note also, that this parametrization differs from a quasi-particle approximation only by one parameter γ_q , and in the limit $\gamma_q \rightarrow 0$ one recovers the free spectral function (5).

Moreover, it may be shown explicitly, that this spectral function has a four-dimensional Fourier transform that vanishes for spacelike coordinate arguments [28]. Since the Fourier transform of the spectral function is nothing but the expectation value of the anti-commutator function of two quark fields, this is an important aspect: It guarantees, that there cannot be any propagation of interactions faster than light. Let us note, that with a general momentum dependence of the spectral width parameter, this requirement may be violated.

For the self energy function we use expressions obtained in a skeleton expansion of the full Green function, i.e., we employ Feynman diagrams for this self energy which are again functionals of the spectral function we wish to determine.

In such an expansion, the one-loop (Fock) diagram, depicted in fig. 1, is the lowest order term with a non-vanishing imaginary part. In the following, we restrict ourselves to this lowest order. We consider a model where quarks are coupled to different types of bosons, to be specified later. The calculation of the Fock self energy with full propagators is straightforward [25] and gives for the imaginary part

$$\begin{aligned} \text{Im}\Sigma^R(p_0, \mathbf{p}) = & \quad (8) \\ & -\pi \int \frac{d^3\mathbf{k}}{(2\pi)^3} \int_{-\infty}^{\infty} dE \Gamma_\mu \mathcal{A}_q(E, \mathbf{k}) \Gamma_\nu \mathcal{A}_B^{\mu\nu}(E - p_0, \mathbf{k} - \mathbf{p}) (n_q(E) + n_B(E - p_0)) . \end{aligned}$$

Here, \mathcal{A}_B is the boson spectral function, Γ_μ and Γ_ν are the interaction matrices at the vertices, and n_B (n_q) is the standard thermal equilibrium Bose (Fermi) distribution functions at temperature T ,

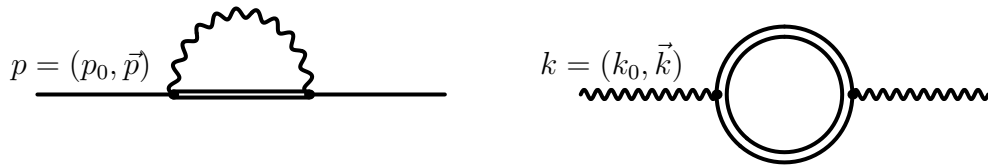


FIG. 1. Self energy diagrams for the photon production rate. Left: Fock diagram for the quark self energy contribution, right: photon polarization diagram including full fermion propagators on both lines.

$$n_{B,q}(E) = \frac{1}{e^{\beta E} \mp 1}. \quad (9)$$

The real part of this self energy function is determined by a dispersion integral, similar to (4) for the propagator. Note, that the divergence of this integral either requires renormalization or a regularization procedure.

Having specified the self-consistency criterion for the quark propagator, we may now ask for its validity. In particular, one may suspect that representing the complicated quark spectral function over the whole range of energies and momenta by only two parameters is an oversimplification. However, we find on the contrary that for the self-consistent Fock approximation with *massless* vector bosons the fermion spectral width is dominated by a constant term [29]. Hence, at low temperatures our ansatz for the spectral function is consistent for quark momenta $|\mathbf{p}| < m_q$.

For higher temperatures the quark mass is small, whereas the quark momenta are typically of the order of the temperature. However, as has been shown in ref. [30], the damping rate is dominated by the minimal distance in the complex energy plane between the origin and the spectral function pole (note, that physical *propagators* do not have poles in the complex plane). This minimal distance is again given by the width, see eq. (29).

For the loop integrals in self energy functions the limitation to small quark momenta is in principle violated. However, equilibrium distribution functions effectively provide a cutoff at momenta $|\mathbf{p}| \simeq T$. We therefore find, and have confirmed this by extensive numerical computations, that the ansatz of a momentum independent spectral width parameter is very well justified for temperatures $T \lesssim \sqrt{m_q^2 + \gamma_q^2}$ – a relation, which is satisfied in our approach. Only in the limit of asymptotic freedom, where the coupling parameters indeed become small, this approximation will possibly fail.

C. Gauge invariant photon production rates

The width calculated from the quark self energy diagram now enters the photon polarization Π at finite temperature, see fig. 1. The imaginary part of the retarded one-loop

polarization function Π^R is [25]

$$\text{Im}\Pi_{\mu\nu}^R(k_0, \mathbf{k}) = -\pi e_q^2 \int \frac{d^3\mathbf{p}}{(2\pi)^3} \int_{-\infty}^{\infty} dE \text{Tr} [\gamma_\mu \mathcal{A}_q(E + k_0, \mathbf{p} + \mathbf{k}) \gamma_\nu \mathcal{A}_q(E, \mathbf{p})] (n_q(E) - n_q(E + k_0)) , \quad (10)$$

where e_q is the electric charge of the quark. The photon production rate for the hot plasma is proportional to this imaginary part, summed over the different physical photon polarization directions.

We now address the question of gauge invariance of the rate calculated in this manner. The photon production rate is gauge invariant if the current which produces the photons is conserved. For the current conserving polarization tensor, which we denote by $\tilde{\Pi}$, this implies transversality, $k^\mu \tilde{\Pi}_{\mu\nu}(k) = 0$.

The polarization tensor Π as calculated from eq. (10), which is connected to the current-current correlator $\Pi_{\mu\nu}(x, y) \propto \langle \bar{\psi}_x \gamma_\mu \psi_x \cdot \bar{\psi}_y \gamma_\nu \psi_y \rangle$, violates this requirement, and may not in general be used for a calculation of the photon production rate.

This can be traced back to the fact, that the naive current $\bar{\psi} \gamma_\mu \psi$ is not conserved. Of course, a theory with a nontrivial spectral function also has a conserved (electromagnetic) current – but this differs from the naive expression [31].

Let us briefly discuss the nature of this difference, starting from the lagrangian of a generalized free field which gives rise to a propagator with certain self energy insertion. A detailed discussion is carried out in ref. [31]. For a one-component fermion field, this would be

$$\mathcal{L}[\psi] = \bar{\psi}(x) (i\partial_\mu \gamma^\mu - m_0) \psi(x) - \int d^4y \bar{\psi}(x) \Sigma(x, y) \psi(y) . \quad (11)$$

Performing a local phase transformation of this field then allows to find a conserved current

$$j^\mu(x) = \bar{\psi}(x) \gamma^\mu \psi(x) - i \int d^4y d^4z \bar{\psi}(z) \Lambda^\mu(z, y; x) \psi(y) . \quad (12)$$

The function Λ^μ is a vertex correction function. Current conservation now is equivalent to the fulfillment of the Ward-Takahashi identity, which for the Fourier transformed quantities reads

$$(p - q)_\mu \Lambda^\mu(p, q) = \Sigma(p) - \Sigma(q) . \quad (13)$$

In this equation, $p - q = k$ is the photon four momentum. Without loss of generality we may fix the photon 3-momentum to be the vector $(0, 0, k)$. It is then obvious, that the Ward identity involves only the components Λ^0 and Λ^3 , it does not restrict the transverse parts Λ^1 and Λ^2 of the vertex correction function. In short words, the logical steps are: Λ^0, Λ^3 nontrivial \Rightarrow transversality of the polarization tensor $\tilde{\Pi} \Rightarrow$ current conservation \Rightarrow gauge invariance of the photon production rate.

Naturally this does not imply, that vertex corrections – if calculated diagrammatically – have only Λ^0, Λ^3 components: It merely tells us, what is *sufficient* to ensure gauge invariance

of the photon production rate. Specifically for the spectral function we have postulated, only Λ^0 is necessary to acquire a conserved current.

Correspondingly only the components $\tilde{\Pi}^{0\nu} = \tilde{\Pi}^{\nu 0}$ of the current conserving polarization tensor are different from the one-loop expression (10). This tensor is the autocorrelation function $\tilde{\Pi}_{\mu\nu} \propto \langle j_\mu j_\nu \rangle$ of the conserved current. It is crucial to realize that the space-like components are not modified, $\tilde{\Pi}^{ij} = \Pi^{ij}$.

In the next step we use this fact together with the condition of on-shell photons, $k_0 = |\mathbf{k}|$. Current conservation implies that $k_0^2 \tilde{\Pi}_{00} = |\mathbf{k}|^2 \tilde{\Pi}_{33}$, i.e., $\tilde{\Pi}_{00} = \tilde{\Pi}_{33}$ for on-shell photons. Hence, these two components cancel in the sum over polarizations:

$$\tilde{\Pi}_\mu^\mu = \tilde{\Pi}^{00} - \tilde{\Pi}^{ii} = \tilde{\Pi}^{00} - \Pi^{ii} = -(\Pi^{11} + \Pi^{22}) . \quad (14)$$

Let us note, that this chain of arguments is rigorous: One may debate, whether vertex corrections are necessary out of phenomenological reasons – but they are *not* necessary in order to achieve a gauge invariant result for the on-shell photon production rate. Of course, this conjecture has a drawback: For the more general case of a momentum dependent spectral function the argument above does not hold any more. Also the calculation of off-shell photon production, such as required for dilepton production rates, necessitates the calculation of vertex corrections.

To summarize this discussion: On the level of our approximate spectral function, and with the fully causal propagators following from this spectral function, the gauge invariant photon emission rate out of the hot plasma is

$$R(E_\gamma, T) = E_\gamma \frac{dN_\gamma}{d^3\mathbf{p}} = 2 \frac{n_B(E_\gamma, T)}{8\pi^3} \text{Im} (\Pi_{11}^R + \Pi_{22}^R) = \frac{i}{8\pi^3} (\Pi_{11}^< + \Pi_{22}^<) , \quad (15)$$

where $\Pi^<$ stands for the off-diagonal component in the standard notation of real-time thermal field theory [25].

The polarization tensor $\Pi(x, y)$ is the correlator of electromagnetic currents at different space-time points. Hence, interference effects between photons emitted from different points in space and time, as far as they affect the single photon rate, are automatically taken into account. This also includes the Landau-Pomeranchuk-Migdal (LPM) effect: Multiple thermal scattering of the slowly moving quarks leads to the interference of sequentially emitted soft photons, thereby reducing the soft photon rate. The equivalence of the semi-classical LPM description with the field theoretical formulation used here has been proven in ref. [11]. We will show that it is exactly this interference effect which gives rise to our primary result.

D. QED plasma and astrophysical consequences

In this subsection, we illustrate the physics with the example of a fermion (quark, or “heavy electron”) interacting electromagnetically in a plasma of temperature T . This can be handled to a large extent analytically and thus allows for a clearer understanding of the mechanism we are treating.

For the purpose of this example, we keep in the following the mass of the fermion fixed at an (arbitrary) value of 300 MeV, and solve the self consistent equation of the in medium

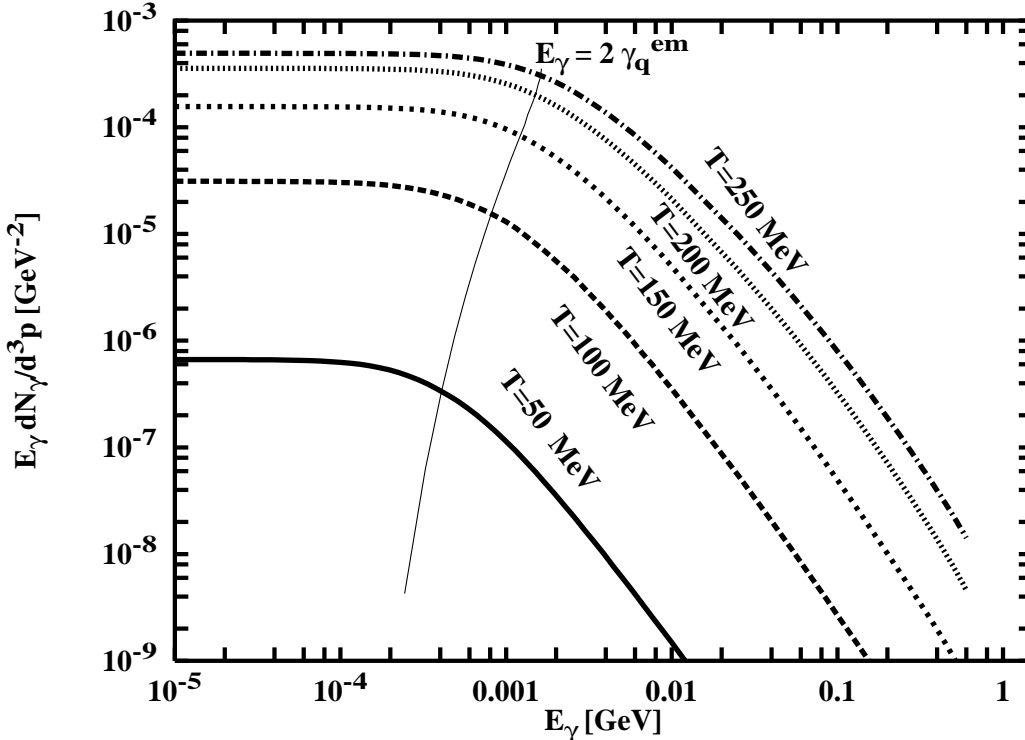


FIG. 2. Photon production rate R_γ from an electromagnetically interacting particle of 300 MeV mass in a plasma as a function of the photon energy E_γ for different temperatures T .

quark propagator, eq.(6), for the width only, using using real and imaginary part of the Fock self energy (8) for massless free photons. The cutoff for the determination of the real part of the self energy function is chosen as $\Lambda + \sqrt{\Lambda^2 + m_q^2}$, with $\Lambda = 650$ MeV (see the discussion in section III.A).

Although this width γ^{em} is, in principle, a non-analytical function of the temperature [29], the smallness of the electromagnetic coupling constant allows to approximate it very well by the lowest order result

$$\gamma_q^{\text{em}}(T) \approx \frac{5}{9}\alpha T \cdot \left[1 - \frac{\text{Re}\Sigma^V}{m_q}\right] \approx \frac{5}{9}\alpha T \cdot \left[1 - \frac{10}{9} \frac{\alpha \Lambda T}{\pi m_q^2}\right] \sim \frac{5}{9}\alpha T, \quad (16)$$

where $\text{Re}\Sigma^V$ is the Lorentz vector ($\propto \gamma^0$) component of the fermion self energy function, and the factor 5/9 is due to the (u,d)- family averaging of electric charge. The purely electrodynamic quark spectral width as function of temperature is plotted in fig. 6, together with the other contributions to be discussed later.

The photon production rate we obtain from eq. (15) with this width is shown in fig. 2 for various typical values of the temperature. For small photon energies, i.e. very soft photons, we find a saturation of the rate below values of $E_\gamma = 2\gamma_q^{\text{em}} \approx 2 \cdot 5/9 \cdot \alpha T$. The factor 2 arises, because the half-maximum width of the Lorentzian spectral function peak is $2\gamma_q$ in our choice of parameters.

The physical interpretation of this effect is obvious: The emission of low-energy photons requires unperturbed propagation of the emitter over the wavelength of the photon. Along

its path however the quark is subject to thermal perturbations – and this hinders the photon emission for for $E_\gamma < 2\gamma_q$. Our result agrees qualitatively with the conjecture of Weldon [10]. Moreover, we could clarify the dominant suppression scale to be twice the spectral width parameter of the emitting particle, or equal to the half-maximum width of the spectral function peak. In the spirit of the last remark in section II.B, we may state that this is an interference effect between photons from different points in space and time.

The rate for high energy photons falls off with photon energy E_γ as $e^{-E_\gamma/T}$ from the Boltzmann factor. For a particle mass $m_q \gg \gamma_q$ this result coincides with previous calculations of eq.(3) with equivalent parameters. However, in contrast to this calculation, our result does not employ singular behavior in the limit of $m_q \rightarrow 0$. This illustrates nicely how the finite thermal particle width regulates the infrared behavior.

The photon production rate may be approximated as

$$R_{\text{fit}}^\gamma = \frac{4\gamma_q}{E_\gamma^2 + 4\gamma_q^2} e^{-E_\gamma/T} z[T] \quad , \quad z[T] \propto \begin{cases} T^2 & \text{for } E_\gamma \ll 2\gamma_q \\ T & \text{for } E_\gamma \gg 2\gamma_q \end{cases} . \quad (17)$$

For all temperatures, the limit $E_\gamma \rightarrow \infty$ is determined by the Boltzmann factor $e^{-E_\gamma/T}$. Note, that this functional dependence is a fitted result after the self-consistent calculation, hence γ_q is not an external parameter that may be varied independently of T and the coupling strength. Numerical fits will be published separately.

Another remark may be appropriate as to compare this result with standard (semi-classical) treatments of the Landau-Pomeranchuk-Migdal effect: Although the exact value of γ_q may be debated, the general form for the radiation rate we obtain conforms very well with all the semi-classical approaches [11,32].

Let us briefly consider the astrophysical consequences of this result. For this we regard an era of the universe, where the photon energy density dominates the matter energy density, roughly $1 \text{ MeV} \leq T \leq 10 \text{ MeV}$. Using eq. (17) together with eq. (16), we find that the photon number density in the early universe is roughly $n_\gamma \approx 2/\pi^2 \cdot T^3$, while the photon energy density is given by $\rho_\gamma \approx 6/\pi^2 \cdot T^4$. These have to be compared to the standard Bose-Einstein values of $n_\gamma^0 \approx 2.4/\pi^2 \cdot T^3$, $\rho_\gamma^0 \approx 6.49/\pi^2 \cdot T^4$. This comparison implies, that the effective number of degrees of freedom, g^* in the total energy density

$$\rho = \frac{\pi^2}{30} g^* T^4 \quad (18)$$

is somewhat reduced by the coherence effects we are considering. This then would lead to a faster expansion of the universe during the time where our result applies. However, this effect is on the order of a few percent and therefore in the moment beyond the reach of experimental observation.

Furthermore we may assume, that in the present spectrum of the cosmic background radiation the photons have retained the spectral cutoff point from the moment when the universe became transparent. If we assume this transition to happen at a temperature of $\approx 1 \text{ eV}$, the effect we are proposing predicts the cosmic microwave background to be thermal at wavelengths shorter than $\lambda_{\text{cut}} = \pi/\alpha T$, but leads to a reduction of the long-wavelength background radiation below its black-body value for larger wavelengths. Due to the expansion factor of $\simeq 1000$, we estimate the present cutoff wavelength to be approximately $\lambda_{\text{cut}} \approx 1 \text{ m}$, which makes it difficult to observe this deviation.

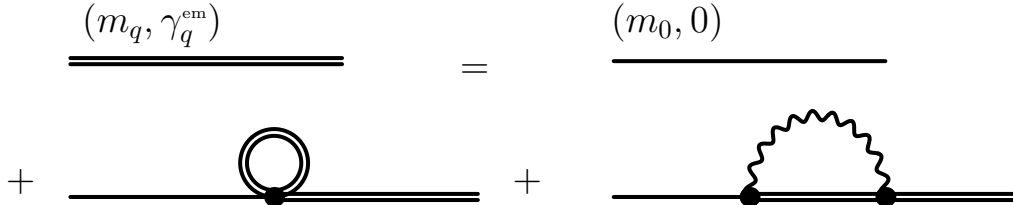


FIG. 3. Diagrammatic equation for the quark propagator at low temperatures. Double line = effective quark propagator, wavy line = photon.

III. PHOTON PRODUCTION FROM A STRONGLY INTERACTING PLASMA

We now come to the main topic of this work, the production of photons from a QGP. For this purpose, we distinguish two temperature regimes. In the low T region, below and around the phase transition temperature, dynamical chiral symmetry breaking and its restoration at $T_c \sim 200$ MeV plays an important role and has to be incorporated in a realistic description of the quark dynamics. We do so by using the Nambu–Jona-Lasinio model as an effective model up to $T \sim T_c$, and add to this model the self-consistent summation of quark-photon Fock diagrams.

In the high temperature limit, chiral symmetry is restored and the coupling is small enough for a perturbative expansion in the strong coupling constant. In this region, we therefore use a self-consistent determination of the quark width obtained in perturbative QCD [33].

In both regimes, nontrivial spectral functions for the respective interacting bosons are used.

A. Nonperturbative temperature regime

Here, we consider the Nambu–Jona-Lasinio model [34] in the SU(2) version on the quark level, see [35] for a review and the notations used in the following.

In this effective field theory, the nonperturbative interaction between quark and antiquark fields at low momentum transfer is described by the sum of a scalar and a pseudoscalar local interaction, $\mathcal{L}_{int} = G[(\Psi(x)\bar{\Psi}(x))^2 + (\Psi(x)i\gamma_5\boldsymbol{\tau}\bar{\Psi}(x))^2]$ where $\Psi = (u, d)$. This is understood to be a summation of nonperturbative gluon interactions among the quark fields. It models the chiral symmetry properties of QCD in the nonperturbative regime, which is essential to address processes on the energy scale of the temperature.

This effective field theory models the chiral symmetry properties of QCD in the nonperturbative regime by a quartic self-interaction of quarks. At small temperature, the dominant contribution to the quark self energy is the tadpole (Hartree) term, which is expressed in terms of the spectral function as [25]

$$\Sigma^H = -2GN_C N_f \int \frac{d^3\mathbf{p}}{(2\pi)^3} \int_{-\Lambda_q}^{\Lambda_q} dE \text{Tr} [\mathcal{A}_q(E, \mathbf{p})] n_q(E). \quad (19)$$

$$\gamma_q^{\text{NJL}} = \gamma_q^{\text{em}} + \text{Im} \left[\text{---} \overset{\sigma}{\text{---}} \text{---} + \text{---} \overset{\pi}{\text{---}} \text{---} \right]$$

FIG. 4. Contributions to the width γ_q of a quark. Short dashed line = scalar meson, long dashed line = pion.

Like any nonrenormalizable model, the NJL requires a momentum cutoff Λ , which can be motivated as a crude incorporation of asymptotic freedom at large Q^2 . For the present generalization, this cutoff is shifted to the energy integration,

$$\Lambda_q = \sqrt{\Lambda^2 + m_q^2(T)}. \quad (20)$$

Usually, the temperature dependent quark mass $m_q(T)$ is the solution of the gap equation $m_q = m_0 + \Sigma^H(m_q)$. With appropriate parameters, this describes the scenario of spontaneous chiral symmetry breaking, i.e., the transition from a current quark mass $m_0 \approx 5$ MeV to the constituent quark mass $m_q \approx 1/3 \times$ the nucleon mass, and its restoration at a transition temperature T_c . The only parameters were chosen as $m_0 = 5$ MeV, $\Lambda = 0.65$ GeV and $G = 5.1$ GeV⁻², and result in $T_c = 193$ MeV and a vacuum mass of $m_\pi = 140$ MeV for the pion and $m_q = 332$ MeV for the constituent quark (135 MeV resp. 331 MeV without photons).

The Fock self energy is the next-to-leading order contribution in a $1/N_c$ expansion [36]. We consider quarks with four-momentum $(p_0, \mathbf{p}) = (m_q, 0)$, hence we can decompose the *retarded* Fock contribution to the self energy in a (complex) scalar and a vector part as $\Sigma^{\text{Fock}} = \Sigma^S + \gamma_0 \Sigma^V$.

The photon Fock contribution is added to the Hartree self energy, and instead of the gap equation we solve eq. (6) for the mass and width of the effective quark field. Split into real and imaginary part this reads

$$\begin{aligned} m_q \gamma_q &= -\text{Im} \Sigma^V(m_q, 0) (m_q - \text{Re} \Sigma^V(m_q, 0)) \\ &\quad - \text{Im} \Sigma^S(m_q, 0) (m_0 + \Sigma^H + \text{Re} \Sigma^S(m_q, 0)) \\ -\gamma_q^2 &= (m_q - \text{Re} \Sigma^V(m_q, 0))^2 - (m_0 + \Sigma^H + \text{Re} \Sigma^S(m_q, 0))^2 \\ &\quad - ((\text{Im} \Sigma^V(m_q, 0))^2 - (\text{Im} \Sigma^S(m_q, 0))^2). \end{aligned} \quad (21)$$

Here, $\text{Im} \Sigma^V$ is an even function of p_0 , $\text{Im} \Sigma^S$ is an odd function of p_0 . For $\gamma_q \rightarrow 0$, the above equations reduce to the standard gap equation of the NJL model.

The NJL model furthermore describes two bound states which are regarded as effective, T -dependent pseudoscalar π -meson and scalar σ -meson.

The traditional way to determine the masses m_B of these collective modes is to solve the equation [35]

$$1 - 2G \operatorname{Re}\Pi(m_B, 0) = 0, \quad (22)$$

with Π the corresponding polarization function determined as a dispersion integral over eq. (10). As a cutoff for the dispersion integral one uses $\pm 2\Lambda_q$ according to eq. (20).

Within our formalism we use the following ansatz for the retarded boson propagator along the real axis:

$$k_\mu k^\mu - m^2 - \Pi^R(k) = (k_0 - (\omega_B(\mathbf{k}) - i\gamma_B)) (k_0 + (\omega_B(\mathbf{k}) + i\gamma_B)) \quad (23)$$

with $\omega_B^2 = m_B^2 + \mathbf{k}^2$. This translates into a spectral function as

$$\mathcal{A}_B(E, \mathbf{k}) = \frac{1}{\pi} \frac{2E\gamma_B}{(E^2 - \Omega_B(\mathbf{k})^2)^2 + 4E^2\gamma_B^2}, \quad (24)$$

with $\Omega_k^2 = \omega_B(\mathbf{k})^2 + \gamma_B^2$.

The parameters m_B and γ_B are determined from the equations

$$\begin{aligned} 1 - 2G \operatorname{Re}\Pi(m_B, 0) + (G \pi \sigma(m_B, 0))^2 &= 0 \\ m_B G \pi \sigma(m_B, 0) &= \gamma_B. \end{aligned} \quad (25)$$

The mesonic Fock contributions to the quark self energy are treated only perturbatively, i.e., their imaginary parts are used to modify the quark width according to fig. 4 and their influence on the quark mass is neglected [36].

To check the consistency of this approximation, we also performed a self consistent summation of the meson Fock diagrams, which gives rise to a small correction of the constituent quark mass as well as the meson masses in our extended NJL model. However, such a summation breaks chiral symmetry explicitly - and one may expect, that the mass shift is canceled by other diagrams. For the purpose of the present paper we therefore chose the perturbative treatment of the meson Fock self energy contributions as described above.

Physically, our approach amounts to consider photon emission processes, which are initiated by the interaction of the quark with a *single* hot meson. The resulting quark width γ_q is plotted in fig. 6. For low temperatures, we again find $\gamma \propto T$ for each channel. Up to a temperature of ≈ 150 MeV, the quark width γ_q is in fact dominated by the purely electrodynamic contribution. This indicates, that photons should be taken into account even for strongly interacting systems at such temperatures.

Due to the quasi-Goldstone mode of the pion, its contribution to the quark width remains negligible up to the Mott temperature $T_M = 212$ MeV, which is defined by $m_\pi(T_M) = 2m_q(T_M)$ as the point where the pion can dissociate in a $q\bar{q}$ pair. For $T > T_M$, the pionic contribution to the quark spectral width is actually dominant. Towards higher temperatures, the competing effect of an increase of the mass of the π (now a resonance) again turns the width down.

One may argue at this point, that in the NJL model quarks are not confined. However, the above results may be translated to other models as well: They represent nothing but a critical opalescence to photons in the vicinity of the chiral phase transition. Hence we expect the drastic increase of the effective γ around T_c to be quite independent of the model used.

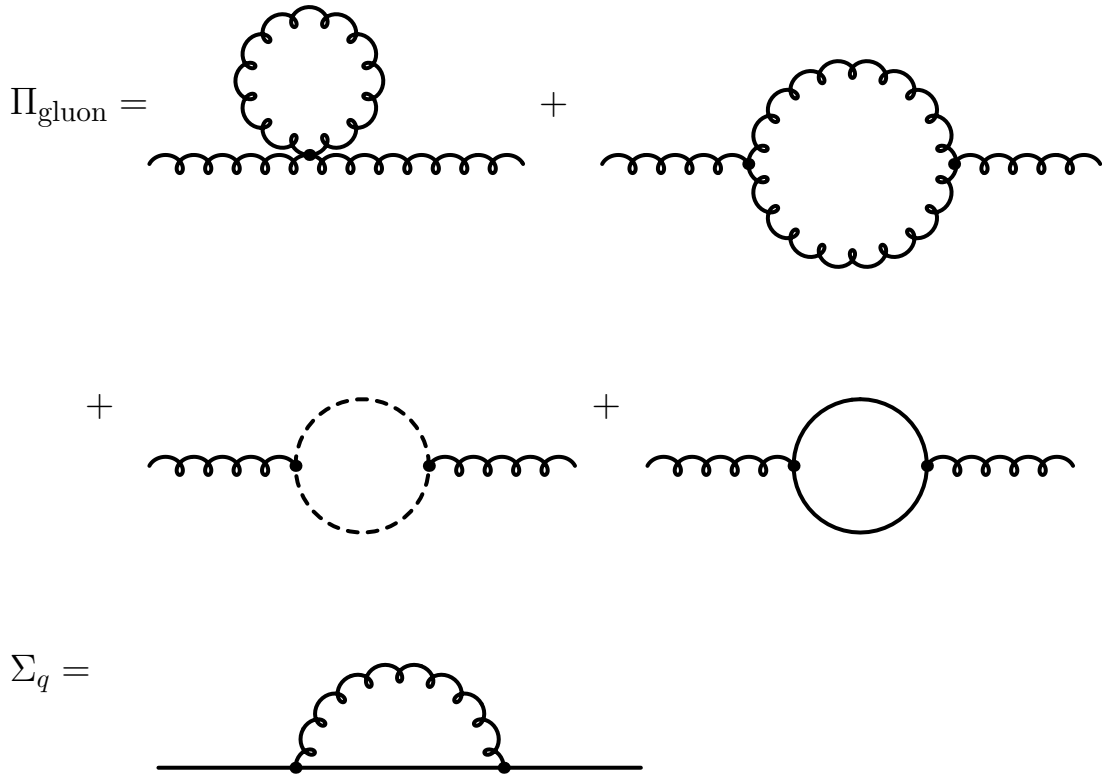


FIG. 5. Feynman diagrams used in the calculation of the effective quark and gluon propagator. Each line represents an effective propagator here, dashed are the ghost fields.

B. Perturbative QCD for high temperature plasma

In the high temperature limit, a calculation within perturbative QCD becomes sensible. Furthermore, non-abelian gauge invariance becomes an imperative of the calculation. For each of the degrees of freedom, i.e., quarks, transverse and longitudinal gluons and ghost fields, one has to consider an effective propagator similar to those we have discussed before.

We will first report on the result of ref. [33], where, in the same spirit as discussed for the electromagnetic case, a high-temperature self-consistent QCD calculation was carried out.

Various self energy diagrams have been taken into account in this work, including – compare this to the QED case – a gluon Fock diagram for the quarks as well as polarization functions for the boson fields. The photon Fock diagram may be neglected in this temperature regime, since its contribution is much smaller than the gluon Fock contribution (see fig. 6). Fig. 5 contains a list of the diagrams, which were self-consistently summed in the infrared limit. Within this calculation, the quark width is obtained as

$$\gamma_q = 0.271 gT \quad (\text{for } N_f = 2, N_c = 3). \quad (26)$$

To the same order of accuracy, and in view of the explanation in section II.B, we use the running coupling constant

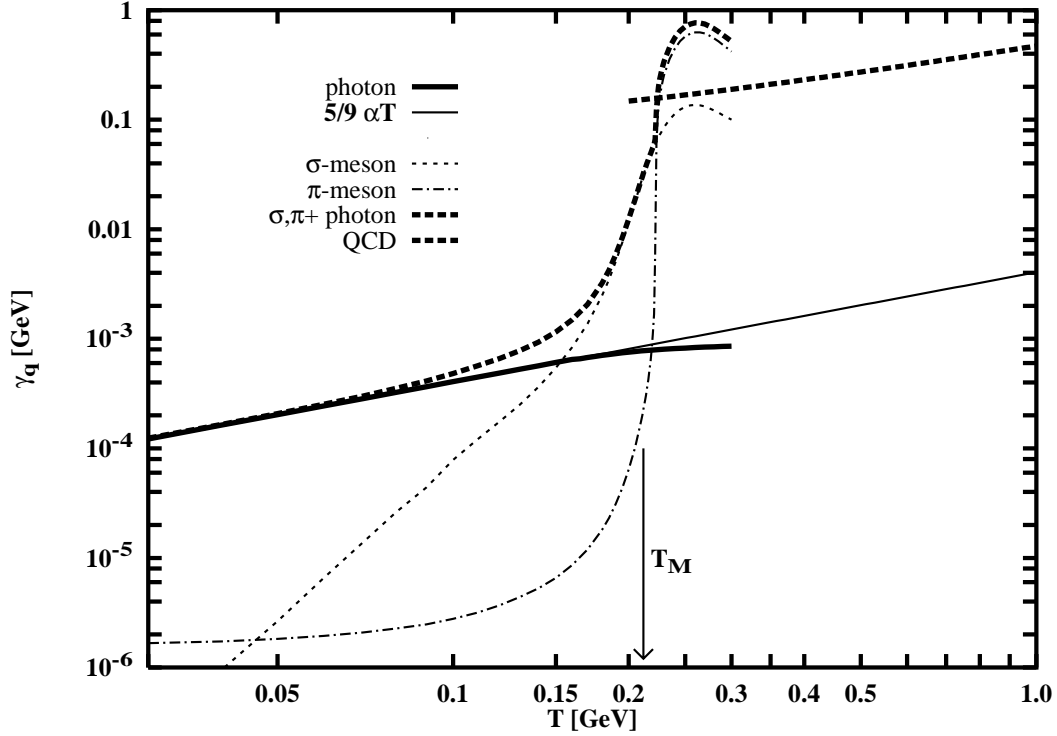


FIG. 6. Contributions to the width γ_q of a quark. Thick dashed line: total quark width, calculated with the NJL model at low temperature and inspired by perturbative QCD at high temperature.

$$g^2(Q^2) = 4\pi \cdot \frac{12\pi}{(33 - 2N_f) \log(Q^2/\Lambda_{\text{QCD}}^2)} \quad (27)$$

with $N_f = 2$ for up and down flavors, only and $\Lambda_{\text{QCD}} = 0.2$ GeV. This gives the proper match to the two-flavor NJL calculation towards low temperatures. Due to their larger current quark mass, the strange quarks will not give a large contribution at the temperatures we consider. We relate the mean Q^2 to the temperature by $\langle Q^2 \rangle \approx (3T)^2$. The resulting quark width reads

$$\gamma_q = \frac{2.858 T}{\sqrt{\log\left[\frac{15.0 \cdot T}{\text{GeV}}\right]}} \approx 1.65 T \text{ for } T \approx 0.2 \text{ GeV}. \quad (28)$$

However, the question remains whether the result $\gamma \propto gT$ does not contradict the calculations in the NJL model, which yielded $\gamma \propto \alpha T \propto e^2 T$. On one hand, we may refer to eq. (33) of [30], where

$$\gamma_q \simeq \frac{3g^2 T^2}{64E_q}. \quad (29)$$

Substituting for E_q the minimal distance between the origin in the complex plane and the pole of the spectral function, i.e., $E_q \simeq \gamma_q$, we find that the self consistent $\gamma_q \simeq 0.216 gT$.

In this framework one would therefore find, that it is the replacement of m_q by γ_q in the infrared screening, which provides a $\gamma_q \propto gT$ instead of g^2T .

On the other hand, there are other calculations within the hard thermal loop resummation method which give a fermion damping rate of order g^2T [20], although one may criticize the propagators used there because they violate the locality axiom of quantum field theory [28].

There, the quark width is obtained as the solution of an equation of the type [20,30,37]

$$\gamma \simeq \frac{g^2}{2\pi^2} T \int_0^{gT} \frac{dk}{k} \arctan\left(\frac{k}{\gamma}\right) = \frac{g^3 T^2}{8\pi^2 \gamma} \Phi\left(-\frac{g^2 T^2}{\gamma^2}, 2, \frac{1}{2}\right), \quad (30)$$

where $\Phi(z, s, a)$ denotes the Lerch transcendent, a generalization of the polylogarithm function and not expressible as a finite series of elementary functions. Numerical evaluation gives a value of

$$\gamma_q \approx 0.82 T \text{ for } T \approx 0.2 \text{ GeV}. \quad (31)$$

For small $g \lesssim 0.5$, one finds

$$\gamma \simeq \frac{g^2}{4\pi} T \log\left(\frac{1}{g}\right) \left(1 - \log\left[\log\left(\frac{1}{g}\right) \frac{1}{4\pi}\right] \left\{\log\left(\frac{e}{g}\right)\right\}^{-1}\right), \quad (32)$$

where e denotes Eulers constant. This is a non-analytical function around the point $g = 0$, but it is *not* of the order $g^2 \log(1/g)$ as claimed in refs. [20,21,37] (this logarithmic piece is also denounced in ref. [30]). Moreover, there are hints that the logarithmic correction is due to a neglect of vacuum parts in the evaluated diagrams [29].

The perturbative spectral width of the quark obtained in the region of the chiral phase transition temperature is also compatible with the high temperature NJL result, which above the Mott transition temperature gives a spectral width of $\gamma \simeq T$.

Hence, starting from three completely different methods: **a.** the NJL model, **b.** effective QCD with generalized free fields and **c.** hard thermal loop resummation, we arrive at similar results $\gamma_q \approx (0.82 \dots 1.65)T$ in the region of the chiral phase transition. Each of these curves matches with the NJL result at temperatures of ≈ 220 MeV, as can be inferred from fig. 6. For reasons to be made clear later we therefore retain the parametrization of eq. (28), but emphasize again that we do not decide at this point whether the quark damping rate is of order gT or g^2T . Rather, we consider this only as a numerical parametrization which is supported by *all* available methods.

The resulting spectral width of the quark is plotted in fig. 6, together with the low temperature result obtained in the previous subsection. This temperature dependent spectral width of the quark therefore has two regions which we consider to be safely established beyond any questions of the detailed model and technique:

$$\gamma_q(T) \simeq \begin{cases} 0.004 \cdot T & \text{for } T \ll T_c \text{ (electromagnetic)} \\ 1.0 \cdot T & \text{for } T \gtrsim T_M \text{ (strong)} \end{cases}. \quad (33)$$

The pronounced rise of the width around the phase transition temperature, which is carried over to a similar rise in the photon rates, is therefore a model independent result of finite temperature QCD. We identify it with the dissociation of the mesons, dominantly $\pi \leftrightarrow q\bar{q}$, which is connected with the phase transition temperature.

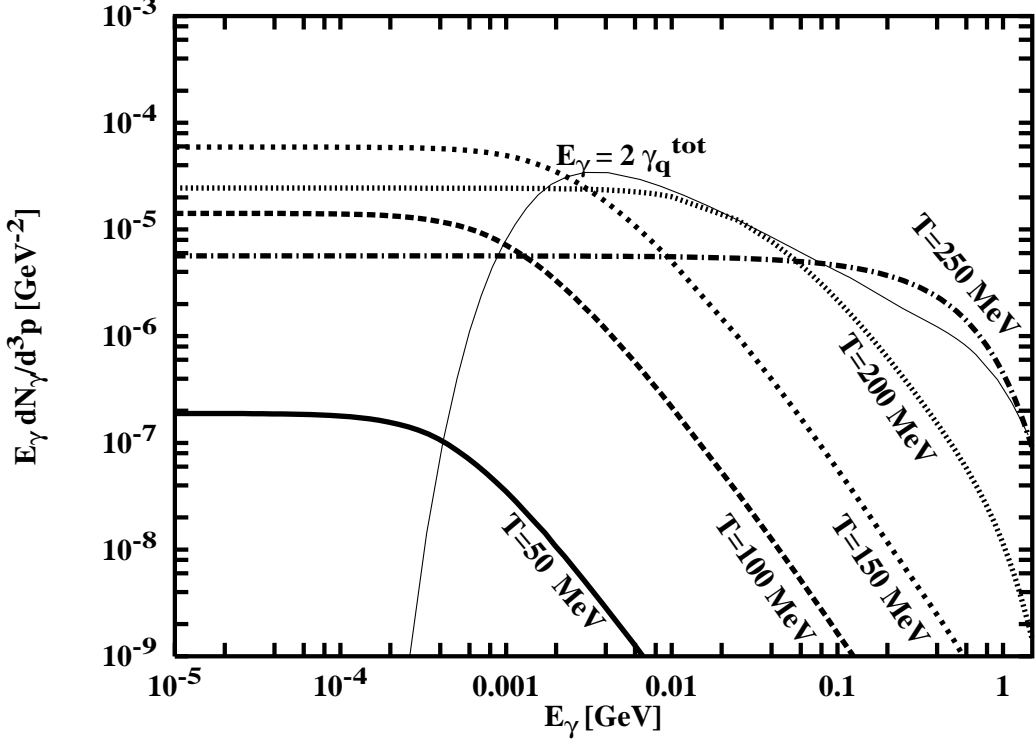


FIG. 7. Photon production rate R as function of the photon energy for different temperatures. Thick lines: Temperatures 50 – 250 MeV (dashed), our calculation using the NJL model. Thin line: Cutoff point $E_\gamma = 2\gamma_q$.

C. Results for photon production rates

First we discuss the photon emission rates obtained from eq.(15) below the chiral phase transition temperature. They are plotted in fig. 7, and we find a great similarity of the rate with the results plotted in fig. 2 for the purely electromagnetic case. However, at temperatures $T > T_M \approx 212$ MeV, the quark width parameter is dominated by the mesonic contributions, which leads to a much higher saturation scale $\gamma_q \gg \gamma_q^{\text{em}}$. In fig. 7 this rise is also documented by the turning of the curve $E_\gamma = 2\gamma_q$, see the thin continuous line.

We now turn to the region of the chiral phase transition. In fig. 8, we compare the NJL calculations at temperature $T=200$ MeV (250 MeV) with the corresponding perturbative QCD calculations. The resulting photon production rates are different at $T=200$ MeV, i.e., very close to the chiral phase transition temperature. The reason for this is clearly, that the perturbative QCD calculation is no longer applicable here.

Very good agreement is reached at a temperature of $T=250$ MeV, which is of course due to the matching values of γ_q at this temperature, see fig. 6.

In fig. 9, we have plotted the perturbative QCD results for temperatures $T=250$ and 400 MeV, i.e., in a region where one would not trust the NJL model. The figure also contains a plot of the photon production rate obtained with the method of hard thermal loops, eq. (3). We find, that our QCD inspired calculation at the lower temperature agrees very well with the NJL result, while at the higher temperature and for hard photons is reproduces the result of the hard thermal loop calculation. For reason of this agreement we have kept

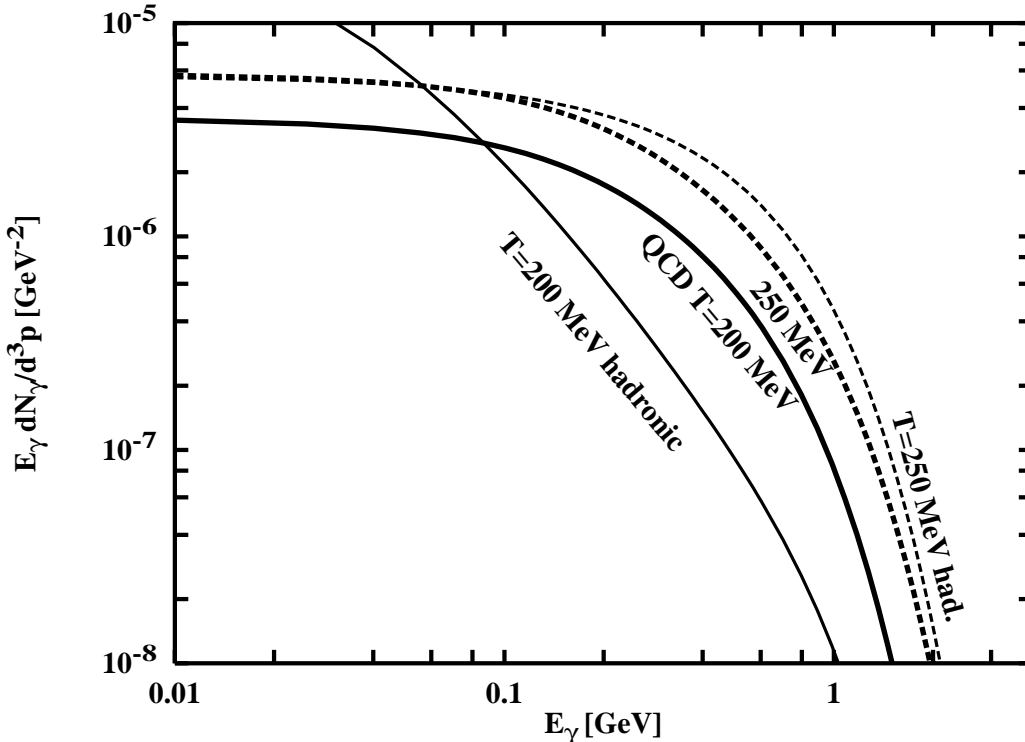


FIG. 8. Photon production rate R from a QGP as function of the photon energy for different temperatures.

Thick lines: $T=200$ and 250 MeV (dashed), our calculation using eq. (28).

Thin lines: $T=200$ and 250 MeV (dashed), our calculation using the NJL model.

our parametrization for the quark spectral width above T_c , eq. (28).

At lower photon energies however, where according to our result the photon radiation is cut off due to the finite mean free path of a particle, the result of the hard thermal loop calculation is not usable. We therefore consider our result an extension of commonly accepted results to a wider range of energies.

The leveling off of the rates at low photon energy is due to the inclusion of coherence (LPM) effects. For lepton pairs, this effect can be compared to the results of ref. [38], where this effect was introduced “by hand”, whereas in our calculation it is automatically included in the formalism.

In fig. 10, we show the photon emission rate at three different photon energies as a function of temperature. Comparing the electromagnetic case (thin lines) to the model including the quark-meson interaction, we find a surprising result: In the region of the chiral phase transition, the low-energy photon production rate *drops* with increasing temperature. Eventually the radiation rate is degenerate for all energies $E_\gamma < 2\gamma_q$ (see the flat behavior of the curves in fig. 7). In view of eq. (17), this is understood as a dominance of the saturation effect over the increase of temperature.

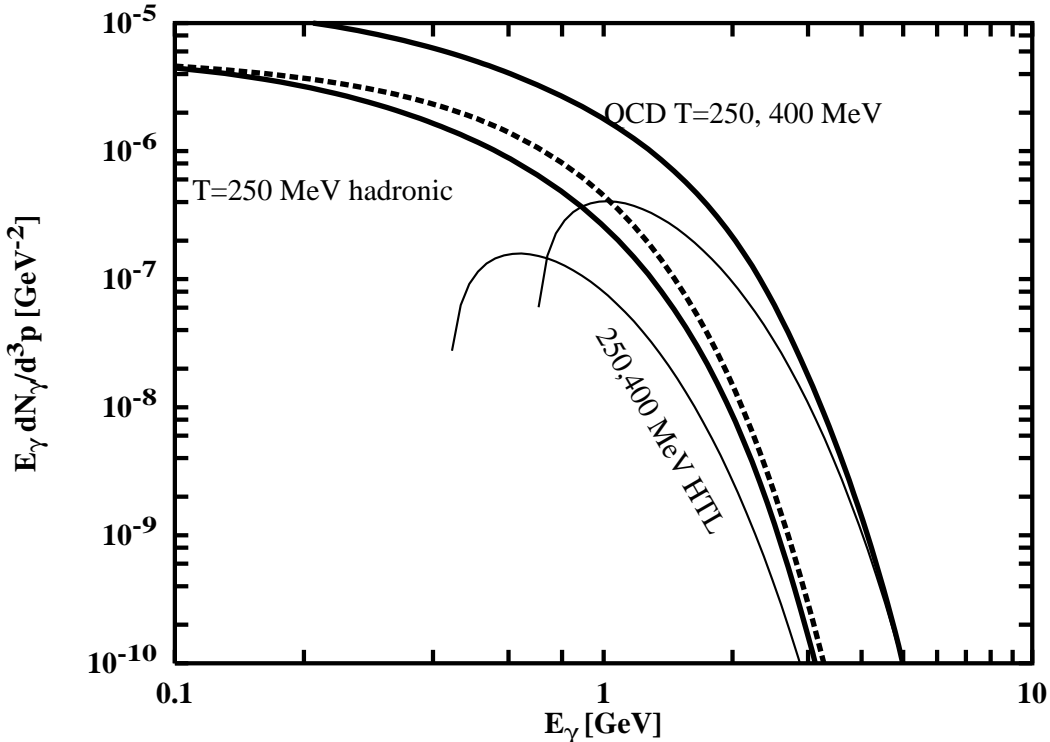


FIG. 9. Photon production rate R from a QGP as function of the photon energy for two different temperatures.

Thick solid lines: $T=250$ and 400 MeV, our calculation using perturbative QCD, eq. (28)

Dashed line: $T=250$ MeV, our calculation using the NJL model

Thin lines: Calculation with the method of hard thermal loops, [7]

D. Relevance to experimental data

We now briefly give an overview of existing or future experiments, in the order of increasing energy, which observe photons in reactions of hadronic character, and discuss the relevance of our rate calculations to them.

Let us first consider very soft (for an experimentalist's scale) photons, where $E_\gamma \sim 1 - 100$ MeV. Photons in this energy region have been measured in several experiments [2–4,39,40]. While some of these experiments find a complete agreement of the measured photon spectra with the emission from hadronic sources and QED bremsstrahlung, an enhancement in the low p_\perp region was observed in reactions such as K^+p [39] and π^-p [40].

At the moment the discussion of experimental results is not yet conclusive, see ref. [41] for an excellent review of the data. However, there is one proposed explanation for such a soft photon excess in case it is present: It might be due to “thermal” radiation of cold drops of quark–gluon plasma, which would hadronize only slowly and thus have a long time to radiate [42,41].

While we think it premature to draw definite conclusions from the puzzling experimental situation, we will comment on the proposed theoretical explanation of an enhanced soft radiation from a cold plasma droplet. Since the emitted photons are soft, the (LPM-) effect of interference between successive emitters is necessarily very strong. Using our results for

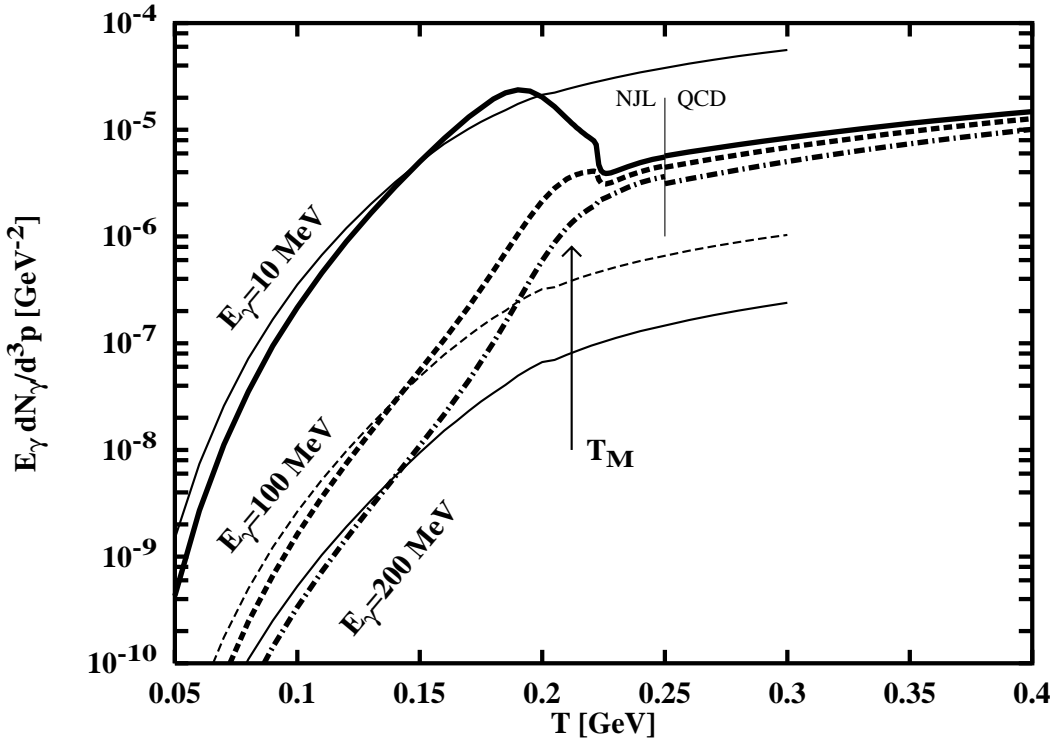


FIG. 10. Photon production rate R from as function of temperature T . Photon energy 10 MeV (solid), 100 MeV (dashed) and 200 MeV (dash-dotted). Thin lines: purely electromagnetic width γ_q^{em} . Thick lines, curves from left: Our calculation using the NJL model. Thick lines, curves from right: Our calculation using perturbative QCD, eq. (28)

the rate as shown in fig. 10, we therefore estimate the expected photon yield from such a cold plasma drop of some size R at a temperature T . From uncertainty, $R \geq 1/\bar{p}$ where \bar{p} is the mean momentum of a plasma particle, and thus cold drops need to be of considerable size. For a drop of volume V and lifetime τ at a temperature T , the differential cross section of photon production at a transverse momentum p_\perp can be expressed as

$$\frac{d\sigma}{dp_\perp} = \frac{V\tau}{(0.2\text{fm})^4} 2\pi p_\perp \sigma_{AB} R(E_\gamma, T) \quad (34)$$

where $R(E_\gamma, T)$ is the invariant rate and σ_{AB} is the total cross section of the reaction $A + B$ under study.

As an example, let us consider the reaction $K^+p \rightarrow \gamma X$ where the p_\perp spectrum of photons was measured [39]. At a temperature of 50 MeV, the invariant rate of photons of say $E_\gamma = 10$ MeV is, reading from fig. 10, about 10^{-9} mb/GeV. Taking a drop lifetime $\tau \sim R \sim 10$ fm and a cross section of $\sigma_{K^+p} = 16$ mb results in an estimate of the photon yield of $d\sigma/dp_\perp \sim 3 \cdot 10^{-2}$ mb/GeV. This is to be compared with the measured value of $d\sigma/dp_\perp|_{\text{exp}} \sim 200$ mb/GeV, which is much larger than the rate estimated from a cold plasma drop emitting photons.

As we noted before, previous calculations in the cold plasma droplet picture had arrived at numbers which correspond to the excess over the bremsstrahlung found in some experi-

ments. However, these calculations do *not* account for the coherence (LPM-) effect which dramatically reduces the rate, and actually the normalization of the spectra obtained in these calculations was taken from experiment. We thus have to conclude, that the mechanism of “thermal” radiation from cold plasma droplets does not account for an excess of soft photons over the bremsstrahlung – independent of the question, whether such an excess is found experimentally or not.

Now consider higher energies of the photon in the range $E_\gamma \geq 100$ MeV. In recent heavy ion experiments at ultrarelativistic energies, it is hoped to find some hints of a phase transition the system might, possibly partially, go through. Apart from measuring photons, experiments also observe lepton pairs which suffer less from coming together with a large background. For both electromagnetic probes, an enhancement might hint at the new phase.

For photons, the invariant rate as shown in figs. 9 and 10 gives our result for the QGP, and needs to be folded with the space-time evolution of the system such as calculated in [8]. For this purpose, the invariant rate may be written in terms of the photon rapidity y and transverse momentum p_\perp as

$$E \frac{d\sigma}{d^3\mathbf{p}} = \frac{1}{2\pi p_t} \frac{d\sigma}{dp_t dy}. \quad (35)$$

Photons with a low virtuality can be converted into dileptons by use of the soft photon approximation,

$$R_{l+l-} = E_+ E_- \frac{dN_{ll}}{d\mathbf{p}_+^3 d\mathbf{p}_-^3} \approx \frac{\alpha}{2\pi^2 M^2} E_\gamma \frac{dN}{d^3\mathbf{k}}, \quad (36)$$

and improved versions thereof [43]. This allows the use of the results presented in this work to the calculation of dilepton rates as well. Again, a space-time integration needs to be performed to compute the yield for a heavy ion reaction at some impact parameter, which is related to the measured multiplicity or total transverse energy.

This integration over the space-time evolution of the collision was performed by use of the photon rates calculated from hard thermal loops [8]. The system proceeds from an initial QGP through a mixed phase to a purely hadronic phase in the final state. Since the initial plasma phase is short-lived and of a similar temperature than later phases under the conditions studied, and the QGP does not shine very much brighter than a mixed or hadronic phase of the same temperature, the yield of photons from the QGP is much smaller than that of the other phases, typically more than an order of magnitude. As can be seen from fig. 9, our results in the range of photon energies $E_\gamma \geq 100$ MeV are similar to those from hard thermal loops which had been used in the analysis [8]. Therefore, the conclusion remains, that the scarce photons from a plasma phase are overwhelmed by those from the later stages of the reaction, and the same is the case for dileptons. This applies to the application of our result to current experiments such as Ceres, WA80/98 and Helios. In particular, an enhancement seen in these experiments can not be accounted for by a direct contribution of the plasma phase, but must be of different origin (which, of course, may still be related to a phase transition).

A substantial transverse flow in these collisions, for which there is some evidence [44], has the tendency to increase the apparent photon energy and thus to increase the photon rates from a QGP [45]. However, we expect that transverse flow has a similar effect on photons

produced from the hot hadron gas in the final stage. Therefore, this effect is probably of no help for the distinction of these photon sources in present measurements.

This situation might change in favor of the quark–gluon plasma when going to higher energies. Here the rate of electromagnetic probes originating in the plasma rises strongly with increasing temperature of the QGP (see fig.9), while the temperature at which the hadronic reactions occur does not change. Experiments which are under preparation at RHIC and LHC are planning to observe photons and dileptons and thus it is hoped that these experiments might see the QGP in sufficiently bright light in order to uniquely identify this phase.

IV. CONCLUSIONS

In this work, we calculated gauge invariant rates for the production of low and high energy photons from a hot plasma in the framework of thermal field theory with generalized free fields. For illustration, we studied a QED plasma and discussed possible astrophysical consequences. The main purpose of this work, the calculation of photon rates from a quark–gluon plasma, was achieved over the entire range of temperatures in a composition of two scenarios. For high temperature, perturbative QCD has been used, while around the chiral phase transition region, the nonperturbative NJL model was employed. Both results were found to match smoothly. This is a very satisfactory result and might be of more general relevance than in this particular case. For high photon energies, our result are similar to those obtained previously in the hard thermal loops technique, which is applicable only in the high temperature regime.

It was one of the main motivations of the present work to demonstrate how meaningful production rates may be obtained at finite temperature for soft photons, where the coherence (LPM) effect plays an important role. We emphasize that the qualitative properties of the soft photon rates, such as the saturation effect towards low temperatures, follow from general physical considerations as we discussed, and are in particular independent of the particular model we used. In particular, the decrease of the production rate of soft photons in the temperature region of the phase transition is a very intriguing result, which also might have observable consequences.

We pointed out that at presently reachable energies, photon production in an ultra-relativistic heavy ion collision is dominated by later phases of the reaction rather than an initially present QGP. However, at the energies of currently planned experiments, the plasma temperatures might be high enough to allow a direct identification of this phase. Here, the precise rate for the production of photons of a given energy as we calculated it is a very important tool for the for the interpretation of the experimental results.

From our results one may furthermore conclude, that quantum field theory in terms of generalized free fields with reasonable parametrizations of spectral functions is a valuable method for the analysis of relativistic heavy ion collisions. The strong gap between quantum field theory as a formalism and its predictive power for *many-body* experiments, which has persisted for some time, is hopefully bridged by the application of *thermal* field theory. We are currently undertaking an effort to derive simple parametrizations of the photon

production rate that might be used as input for simulation codes.

Acknowledgments:

We would like to thank J.Hüfner, J.Kapusta, J.Knoll and W.Weise for valuable discussions and suggestions. To D.Srivastava we owe our thanks for pointing out the problem of soft photons, and to H.J.Specht for clarifying this problem in a critical discussion.

REFERENCES

- [1] Quark Matter 95 Proceedings, Nucl. Phys. **A590**, 3c (1995); Quark Matter 93 Proceedings, Nucl. Phys. **A566**, 1c (1994)
- [2] J.Antos et.al., Z.Phys. **C59** (1993) 547
- [3] WA80 Collab., R.Santo et al., Nucl. Phys. **A566**, 61c (1994); T.Awes et al., Nucl. Phys. **A590**, 81c (1995)
- [4] CERES Collab., R. Baur et al., ‘Search for direct photons from S–Au collisions at 200-GeV/u’, CERN-PPE-95-116, Aug. 1995
- [5] Helios–3 Collab., M.Masera, Nucl. Phys. **A590**, 93c (1995)
- [6] CERES Collab., G. Agakichiev et al., ‘Enhanced Production of Low Mass Electron Pairs in 200-GeV/U S - Au Collisions at the CERN SPS’, CERN-PPE-95-26, March 1995; I.Tserruya, Nucl. Phys. **A590**, 127c (1995)
- [7] J.Kapusta, P.Lichard and D.Seibert, Phys.Rev.**D44**, 2774 (1991)
- [8] D.K.Srivastava and B.Sinha, Phys. Rev. Lett. **73**, 2421 (1994); J.Neumann, D.Seibert and G.Fai, Phys. Rev. **C 51**, 1460 (1995); N.Arbex, U.Ornik, M.Plümer, A.Timmermann and R.Weiner, Phys. Lett. **B 345**, 307 (1995); A.Dumitru, U.Katscher, J.Maruhn, H.Stöcker, W.Greiner and D.Rischke, Phys. Rev. **C 51**, 2166 (1995)
- [9] J.Kapusta, D.Kharzeev and L.McLerran, CERN–TH/95–168, hep-ph/9507343; Z. Huang and X.-N. Wang, hep-ph/9507395
- [10] H.A.Weldon, Phys. Rev. **D 49**, 1579 (1994)
- [11] J.Knoll and D.Voskresensky, Phys. Lett. **B351**, 43 (1995) and GSI-Preprint 95-63, hep-ph/9510417
- [12] P.A.Henning and E.Quack, Phys. Rev. Lett. **75**, 2811 (1995)
- [13] P.Aurenche, R.Baier, M.Fontannaz and D.Schiff, Nucl. Phys. **B286**, 509 (1987); **B297**, 661 (1988); P.Aurenche, R.Baier and M.Fontannaz, Phys. Rev. **D42**, 1440 (1990)
- [14] J.Cleymans, E.Quack, K.Redlich and D.Srivastava, Int. J. Mod. Phys. **A10**, 2999 (1995)
- [15] J.Huston, E.Kovacs, S.Kuhlmann, H.Lai, J.Owens and W.Tung, Phys. Rev. **D 51**, 6139 (1995)
- [16] E.Quack and D.Srivastava, GSI-Preprint 95–40, hep-ph/9508217
- [17] R.C.Hwa and K.Kajantie, Phys.Rev. **D 32**, 1109 (1985)
- [18] R.D.Pisarski, Phys. Rev. Lett. **63**, 1129 (1989), E.Braaten and R.D.Pisarski, Nucl. Phys. **B 337**, 569 (1990)
- [19] R.Baier, H.Nakkagawa, A.Niegawa and K.Redlich, Z.Phys. **C 53**, 433 (1992)
- [20] R.Baier, S.Peigné and D.Schiff, Z.Phys. **C62** (1994) 337
- [21] P.Aurenche, T.Becherrawy and E.Petitgirard, hep-ph/9403320, 1994
- [22] H.Narnhofer, M.Requardt and W.Thirring, Commun.Math.Phys. **92**, 247 (1983)
- [23] R. Kubo, J.Phys.Soc. Japan **12**, 570 (1957); C.Martin and J.Schwinger, Phys.Rev. **115**, 1342 (1959)
- [24] R.L.Kobes and G.W.Semenoff, Nucl.Phys. **B260**, 714 (1985) and **B272**, 329 (1986)
- [25] P.A.Henning, Phys.Rep. **253**, 235 (1995)
- [26] H.J.Borchers and R.N.Sen, Commun. Math. Phys. **21**, 101 (1975)
- [27] N.P.Landsman, Ann.Phys. **186**, 141 (1988)
- [28] J.Bros and D.Buchholz, Z.Physik **C 55** (1992) 509 and hep-th 9511022; P.A.Henning, E.Poliatchenko and T.Schilling, GSI-preprint 95-70, hep-ph 9510322
- [29] P.A.Henning, R.Sollacher and H.Weigert, GSI-Preprint 94-56 (1994), hep-ph/9409280

- [30] S.Peigné, E.Pilon and D.Schiff, Z.Physik **C60** (1993) 455
- [31] P.A.Henning and M.Blasone, GSI Preprint 95-36 (1995), hep-ph 9507273
- [32] J.Cleymans, V.V.Goloviznin and K.Redlich, Phys.Rev. **D47** (1993) 989
- [33] P.A.Henning and R.Sollacher, GSI Preprint 95-04 (1995), hep-ph 9501203
- [34] Y. Nambu and G. Jona-Lasinio, Phys. Rev. 122, 345 (1961) and 124, 246 (1961)
- [35] S.P.Klevansky, Rev.Mod.Phys. **64**, 649 (1992)
- [36] E.Quack and S.P.Klevansky, Phys. Rev. **C 49**, 3283 (1994); P.Zhuang, Phys. Rev. **C 51**, 2256 (1995)
- [37] R.Baier and R.Kobes, Phys. Rev. **D 50** (1994) 5944
- [38] J.Cleymans, V.Goloviznin and K.Redlich, Z.Phys. **C 59**, 495 (1993)
- [39] P.Chliapnikov et al., Phys. Lett. **B 141**, 276 (1984)
- [40] S.Banerjee et al., Phys. Lett. **B 305**, 182 (1993) and references quoted here
- [41] P.Lichard, Phys.Rev. **D50** (1994) 6824
- [42] L.Van Hove, Ann.Phys. (NY) 192, 66 (1986); P.Lichard and L.Van Hove, Phys. Lett. **B 245**, 605 (1990)
- [43] R.Rückl, Phys. Lett. **B 64**, 39 (1976); P.Lichard, Phys.Rev.**D 51**, 6017 (1995)
- [44] E.Schnedermann and U.Heinz, Phys. Rev. Lett. **69**, 2908 (1992)
- [45] J.Alam, D.K.Srivastava, B.Sinha, D.N.Basu, Nucl. Phys. **A566**, 343c (1994)

